Cell

Crystal Structure of the TLR4-MD-2 Complex with Bound Endotoxin Antagonist Eritoran

Ho Min Kim,[1,7] Beom Seok Park,[1,7] Jung-In Kim,[1] Sung Eun Kim,[1] Judong Lee,[2] Se Cheol Oh,[1] Purevjav Enkhbayar,[4] Norio Matsushima,[5] Hayyoung Lee,[6] Ook Joon Yoo,[2] and Jie-Oh Lee[1,3,*]
[1]Department of Chemistry
[2]Biomedical Research Center
[3]Institute for Bio-Century
Korea Advanced Institute of Science and Technology, Daejon, Korea 305-701
[4]Faculty of Biology, National University of Mongolia, Ulaanbaatar, Mongolia
[5]School of Health Sciences, Sapporo Medical University, Sapporo, Japan 060-8556
[6]Department of Biology, School of Bioscience & Biotechnology, Chungnam National University, Daejon, Korea 305-764
[7]These authors contributed equally to this work.
*Correspondence: jieoh.lee@kaist.ac.kr
DOI 10.1016/j.cell.2007.08.002

SUMMARY

TLR4 and MD-2 form a heterodimer that recognizes LPS (lipopolysaccharide) from Gram-negative bacteria. Eritoran is an analog of LPS that antagonizes its activity by binding to the TLR4-MD-2 complex. We determined the structure of the full-length ectodomain of the mouse TLR4 and MD-2 complex. We also produced a series of hybrids of human TLR4 and hagfish VLR and determined their structures with and without bound MD-2 and Eritoran. TLR4 is an atypical member of the LRR family and is composed of N-terminal, central, and C-terminal domains. The β sheet of the central domain shows unusually small radii and large twist angles. MD-2 binds to the concave surface of the N-terminal and central domains. The interaction with Eritoran is mediated by a hydrophobic internal pocket in MD-2. Based on structural analysis and mutagenesis experiments on MD-2 and TLR4, we propose a model of TLR4-MD-2 dimerization induced by LPS.

INTRODUCTION

Innate immunity provides immediate and efficient defense against microbial infection. It promotes inflammatory responses and also plays a role in the induction of the adaptive immune system that recognizes specific antigens. Toll-like receptors (TLRs), a family of type I transmembrane glycoproteins, are central to vertebrate innate immune responses (Gay and Gangloff, 2007; Medzhitov et al., 1997). They recognize broad but highly conserved structural patterns on bacteria, fungi, and viruses, which are generally absent from host molecules and are called pattern recognition receptors. To date, 13 mammalian members of the TLR family have been identified, and six subfamilies have been defined based on function and sequence characteristics (Matsushima et al., 2007; Roach et al., 2005). The extracellular segments of TLRs consist of leucine-rich repeats (LRR) with horseshoe-like shapes (Gay and Gangloff, 2007). Binding of ligands to the extracellular domains of TLRs causes a rearrangement of the receptor complex and triggers the recruitment of specific adaptor proteins to the intracellular domain, thus initiating a signaling cascade.

TLR4 is composed of a 608 residue extracellular domain, a single transmembrane domain, and a 187 residue intracellular domain (Medzhitov et al., 1997). MD-2, which lacks transmembrane and intracellular regions, associates with the extracellular domain of TLR4 and is believed to be the component of the TLR4-MD-2 complex that interacts with LPS (lipopolysaccharide) (Shimazu et al., 1999; Viriyakosol et al., 2001). LPS is an outer membrane glycolipid of Gram-negative bacteria and a well-known inducer of the innate immune response (Raetz and Whitfield, 2002). It is composed of a hydrophobic lipid A component and the hydrophilic polysaccharides of the core and O-antigen. The lipid A portion, which is composed of phosphorylated di-glucosamine and multiple acyl chains, corresponds to the conserved molecular pattern of LPS and is the main inducer of biological responses to LPS. LPS is extracted from the bacterial membrane and transferred to TLR4 by two accessory proteins, LPS-binding protein (LBP) and CD14 (Miyake, 2006).

TLR4 and MD-2 are essential for LPS recognition. The C3H/HeJ strain of mice, which tolerates lethal doses of LPS and has altered inflammatory responses, was found to have a missense mutation in the conserved region of

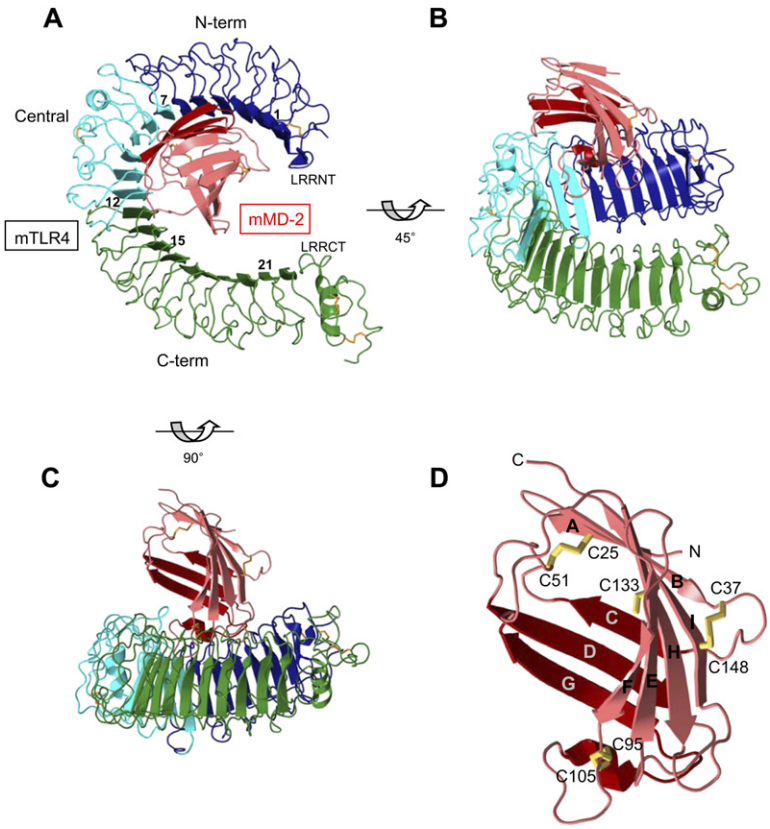

Figure 1. Overall Structure of the Mouse TLR4-MD-2 Complex

(A–C) Three views of the mouse TLR4-MD-2 complex are shown in the diagrams. The N-terminal, central, and C-terminal domains of TLR4 are colored in blue, cyan, and green, respectively. The beta strands of MD-2 are shown in pink and red, and the LRR modules of TLR4 are numbered.

(D) Closeup view of mouse MD-2. Disulfide bridges are shown in yellow and cysteines are labeled. Cys133 is not involved in the disulfide bridge formation. The orientation of this view is the same as for (C).

the TLR4 intracellular domain (Poltorak et al., 1998; Qureshi et al., 1999). Similar tolerance was observed in the C57BL/10ScCr mutant, which has a deletion of the entire *tlr4* locus, and in TLR4-deficient mice (Hoshino et al., 1999; Poltorak et al., 1998; Qureshi et al., 1999). However, transfection of TLR4 alone is not enough for LPS recognition, and physical association of TLR4 with MD-2 on the cell surface is a prerequisite for ligand-induced activation (Nagai et al., 2002; Schromm et al., 2001; Shimazu et al., 1999). LPS has similar affinity for MD-2 as for the TLR4-MD-2 complex, demonstrating that MD-2 is the LPS-binding component (Viriyakosol et al., 2001). Only the monomeric form of soluble recombinant MD-2 was found to bind LPS, producing a stable MD-2-LPS complex, and this complex was sufficient for inducing TLR4-dependent activation (Gioannini et al., 2004; Re and Strominger, 2002).

Engagement of LPS on the host cell activates a strong immune response that protects the human body against further infection. However, it can also lead to a fatal septic syndrome if the inflammatory response is amplified and uncontrolled. Eritoran (or E5564) is a synthetic molecule derived from the lipid A structure of the nonpathogenic LPS of *Rhodobacter sphaeroides* (Mullarkey et al., 2003; Rossignol and Lynn, 2005). It is a strong antagonist of TLR4-MD-2 and is currently in a phase III clinical trial for severe sepsis. Although the first crystal structures of TLR3 was recently reported (Bell et al., 2005; Choe et al., 2005), the structural basis of ligand binding and activation of TLR family proteins still remain to be clarified. To address these questions, we undertook structural studies of TLR4-MD-2 and its complex with Eritoran.

RESULTS

Structure of Mouse TLR4

To determine the structure of the mouse TLR4-MD-2 complex, the full-length ectodomains of mouse TLR4 and MD-2 were expressed in cultured insect cells using recombinant baculoviruses. The mouse TLR4 and MD-2 proteins form a stable 1:1 complex and are not separated during purification. In the crystal structure, one molecule of MD-2 binds to each TLR4, confirming previous reports that only monomeric MD-2 interacts with TLR4 and mediates LPS signaling (Figure 1) (Gioannini et al., 2004, 2005; Re and Strominger, 2002).

The crystal structure shows that TLR4 is an unusual member of the "typical" subfamily of the LRR superfamily. Typical subfamily LRR proteins have characteristic horseshoe-like structures whose concave surface is formed by parallel β strands and whose convex surface is formed by loops and 3_{10} helices (Kajava, 1998; Kobe and Kajava, 2001). The parallel β sheet of the typical subfamily has uniform twist angles and radii throughout the entire protein. Unlike other typical family members including TLR3, analysis of the β sheet conformation of TLR4 demonstrates

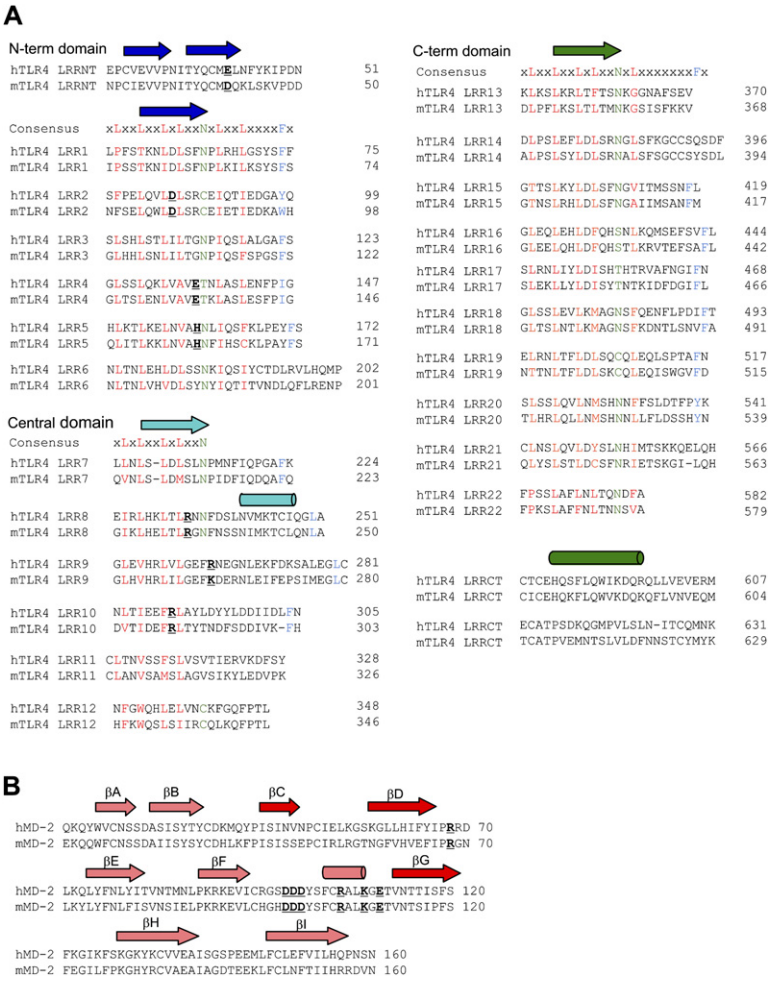

Figure 2. Sequence Alignments and Secondary Structure Assignments of TLR4 and MD-2

(A) Structure-based alignment of human and mouse TLR4 sequences. β strands and α helices of the TLR4 and MD-2 are shown above the sequence alignment as arrows and cylinders, respectively. Residues involved in the asparagine ladder and phenylalanine spine are colored green and cyan, respectively. Residues important for the MD-2 interaction are in bold and underlined.

(B) Sequence alignment and secondary structure assignment of human and mouse MD-2. β strands in the two β sheets are colored pink and red, respectively. Residues involved in TLR4 binding are written in bold and underlined.

that it can be divided into N-, central, and C-terminal domains and undergoes sharp structural transitions at the domain boundaries (Figures 1A–1C and S1 and Table S1).

The N-terminal domain starts from amino acid residue 26 and ends at residue 201 and contains the LRRNT module and LRR modules 1 to 6 (Figure 2). The LRRNT module has no sequence homology with the LRR modules and protects the otherwise exposed hydrophobic cores of the LRR modules. The sequences of the six LRR modules in the N-terminal domain agree well with the conserved pattern of LRR modules of the typical subfamily. The radius and twist angle of the N-terminal domain also agree well with those of typical LRR subfamily members (Table S1). The C-terminal domain of TLR4 contains the LRRCT module and LRR modules 13 to 22. The radius of the β sheet of the C-terminal domain is 28% larger than that of the N-terminal domain. Like LRRNT, the LRRCT module contains two disulfide bonds and covers the hydrophobic core of the LRR modules at the C terminus.

The central domain is composed of LRR modules 7 to 12 and has a 35% smaller radius and three times greater twist angles than those of TLR3 (Table S1). It includes the "hypervariable" region that is essential for recognition of an LPS variant from *P. aeruginosa* (Hajjar et al., 2002). The conformational variation of the central domain appears to originate from three changes in its sequence conservation pattern (Figure 2). (1) The standard LRR module contains two variable amino acids between the first and second conserved leucines. However, the LRR modules of the central domain have only one variable residue. (2) Signature residues important in the structure of the "typical" subfamily LRR proteins are missing from the central domain. In the typical subfamily, the conserved asparagines form a continuous hydrogen-bonding ladder and the phenylalanines form a hydrophobic spine (He et al., 2003; Kim et al., 2007). In TLR4, the asparagine ladder is absent from LRR modules 9 ~12 and the phenylalanine spine is broken at the border between the central and the C-terminal domain. (3) The lengths of the LRR modules of the central domain vary considerably, ranging from 20 to 30 amino acid residues. The length of the LRR module is strongly correlated with the overall shape of the horseshoe-like structure. The LRR superfamily consists of six subfamilies, within which the lengths of the LRR modules

are conserved (Kajava, 1998; Kobe and Kajava, 2001). Subfamilies with shorter LRR modules have loops in their convex regions, and those with longer ones have α-helical structures. Since an α helix requires more space than loops, the horseshoe-like structures with longer LRR modules have smaller radii. Thus the large variation in the length of the LRR modules appears to affect the radius and shape of the horseshoe-like structure of the central domain.

Structure of Mouse MD-2

MD-2 adopts a β cup fold with two antiparallel β sheets that contain three and six β strands, respectively (Figure 1D). The β cup fold is different from the immunoglobulin fold although both of them contain sandwiched antiparallel β sheets (Derewenda et al., 2002; Friedland et al., 2003; Wright et al., 2003). In the β cup fold, the two β sheets become separated on one side of the protein and the hydrophobic internal core is open for ligand binding. Furthermore, the conserved disulfide bridge that connects the two β sheets in the immunoglobulin fold is absent from the β cup so that the two sheets can be separated, further permitting the formation of a large internal pocket. The MD-2 pocket is narrow and deep with a total surface area of 1000 Å^2. The overall shape and chemical behavior of the pocket appear to be suitable for binding large flat molecules such as LPS that contain multiple hydrophobic acyl chains and negatively charged phosphate groups. The generous internal surface of the pocket is completely lined with hydrophobic residues, and the opening region of the pocket contains positively charged residues that facilitate the binding of LPS.

Unlike the majority of globular proteins, MD-2 does not have a sizable hydrophobic core because almost all of its hydrophobic residues are involved in forming the internal pocket. Therefore other structural elements appear to have a more important effect on the stability of the protein. The disulfide bridge connecting Cys25 and Cys51, together with hydrogen bonds between Tyr34, Tyr36, and the backbone atoms of the βC strand, close the bottom of the pocket and stabilize the cup-like structure (Figure 1D). The remaining two disulfide bridges buttress structures of the loops connecting the β strands.

Interaction between TLR4 and MD-2

The surface of TLR4 that interacts with MD-2 has a long and narrow shape with dimensions 40 × 20 Å (Figure 3A). It can be divided into two chemically and evolutionarily distinct areas, the A and B patches. The A patch is negatively charged and evolutionarily conserved, whereas the B patch is positively charged and located in a less conserved area, although the residues directly interacting with MD-2 are strictly conserved (Figures 3B and 3C). The A and B patches of TLR4 are composed of the residues in the concave surface derived from the "LxLxxN" part of the LRR modules in the N-terminal domain and of the central domain, respectively (Figure 2). The interaction between TLR4 and MD-2 is mediated by an extensive network of charge-enhanced hydrogen bonds (Figure 3A). The negatively charged residues in the A patch interact with the positively charged Arg68 and Lys109 residues in MD-2. The positively charged B patch interacts with negatively charged residues in the loop between the βF strand and the α helix of MD-2. The parts of MD-2 interacting with the A and B patches of TLR4 are named the A′ and B′ patches, respectively, in Figure 3. The large interaction area and the complementary charge distribution over the

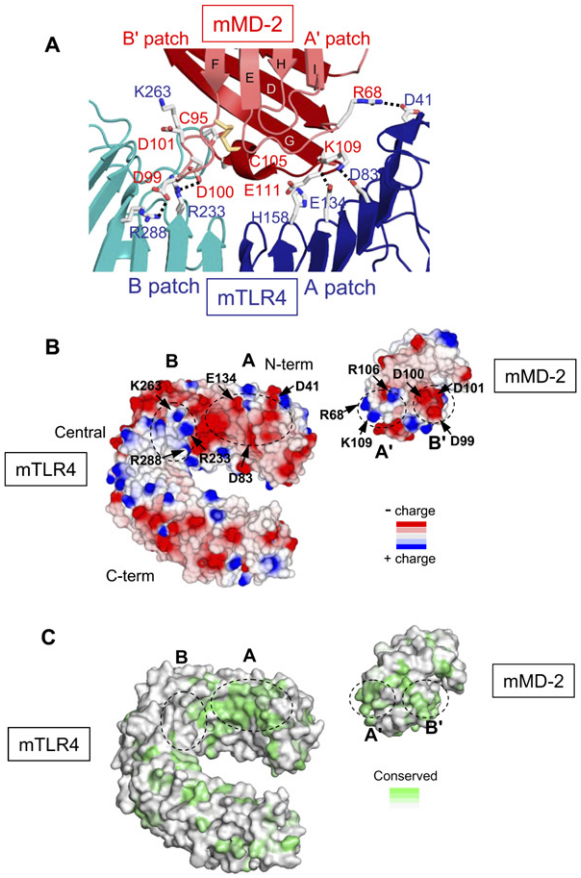

Figure 3. Interactions between TLR4 and MD-2

(A) Closeup view of the interaction region between TLR4 and MD-2. Residues involved in the interaction are labeled. The disulfide bridges are shown in yellow. Hydrogen bonds are drawn with broken lines. Hydrogen bond distances are 3.1, 2.5, 3.1, 2.9, and 2.9 Å for the R68-D41, K109-D83, E111 backbone-E134, D100-R233, and D99-R288 pairs, respectively.

(B) Electrostatic potentials of TLR4 and MD-2. The surface potential was calculated and displayed using the CCP4 mg program (Potterton et al., 2004). The interaction patches of TLR4 and MD-2 are circled and labeled. The orientation of the view of TLR4 is similar to that of Figure 1B. In order to show the binding surface, MD-2 is rotated 180 degrees along the vertical axis.

(C) Sequence conservation of TLR4 and MD-2. Conservation scores were calculated by the Bayesian method using the Consurf server (Landau et al., 2005). Residues directly involved in the TLR4-MD-2 interaction are strictly conserved except for Asp41 and Lys263 of TLR4, which are conservatively changed to glutamates and arginines, respectively, in some species.

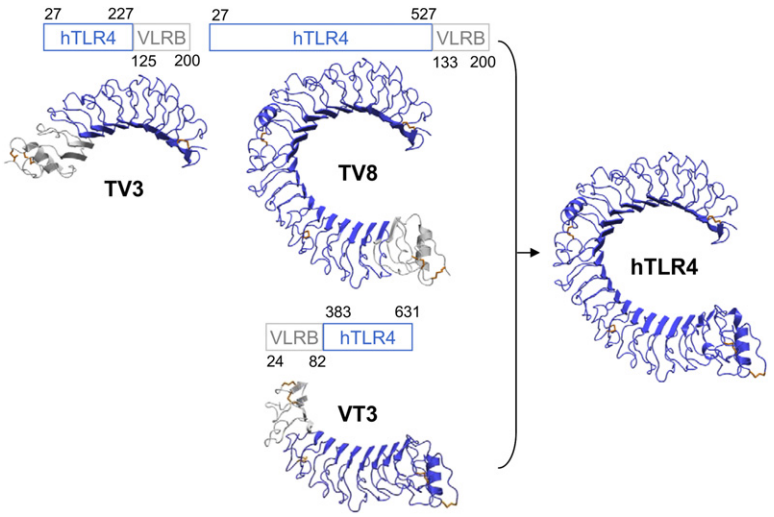

Figure 4. Assembly of the Full-Length Ectodomain of Human TLR4

Structures of the three human TLR4-VLRB.61 hybrids. TLR4 fragments are colored blue and VLRB.61 fragments gray. The full-length ectodomain of human TLR4 was assembled after superimposition of the overlapping regions of the TV8 and VT3 hybrids. The disulfide bridges are represented in orange.

interaction surface are consistent with the nanomolar binding affinity of TLR4-MD-2 (Hyakushima et al., 2004).

Previous reports support our structural observations. Nishtani et al. have shown that mutations of TLR4 residues Cys29 and Cys40, and a synthetic peptide including the residues from Glu24 to Lys47 of TLR4, block TLR4 binding to MD-2 (Nishitani et al., 2005, 2006). This region is not only important for the structural integrity of the LRRNT module but also contains Asp41, a crucial component of the A patch of TLR4. Mutations of MD-2 residues Cys95, Cys105, Asp99, Asp100, and Asp101 in the B′ patch have also been shown to disrupt TLR4 binding (Re and Strominger, 2003).

Designing Hybrids of Human TLR4 and Hagfish VLR

To facilitate soluble expression and crystallization of the TLR4-MD-2 complex with bound ligands, we have developed a novel technique that we term the "Hybrid LRR Technique" in this article. Difficulties in producing target proteins in soluble form and in crystallizing them are the two most common obstacles to successful crystallographic studies. These problems can sometimes be bypassed by removing nonessential domains because many proteins have multiple domains linked by flexible loops, and biological function is often dependent on domains much smaller than the full-length protein. All natural LRR proteins including TLR4 have two specialized modules, LRRNT and LRRCT, that cover the otherwise exposed central hydrophobic core of the LRR modules (Kajava, 1998; Kobe and Kajava, 2001). Truncation of the LRR modules in a target protein will also remove these structurally indispensable LRRNT or LRRCT modules. To avoid this problem we fuse truncated fragments of TLR4 with the LRRNT or LRRCT modules from other LRRs. The VLR proteins of hagfish were chosen as fusion partners because all VLR proteins have canonical LRR structures with sequence diversity in their variable regions maximized (Kim et al., 2007). Therefore good fusion partners can be selected from a large pool of diverse VLR proteins. By varying fusion partners and the site of fusion of pairs of proteins, this technique can generate a practically unlimited number of hybrid LRR proteins without loss of structural integrity.

After many unsuccessful attempts we realized that the "LxxLxLxxN" regions of the LRR modules would be the best fusion sites because they are highly conserved and their structures are practically invariant (Kajava, 1998; Kobe and Kajava, 2001) so that one can predict the structure of the resulting hybrid proteins with great confidence. Relative positions of the conserved residues were strictly preserved at the fusion sites (Table S2). This fusion strategy was surprisingly successful, such that of 15 fusion proteins designed, 7 yielded soluble hybrids (Table S2). Some of the hybrids were tested and found to bind MD-2 and to yield crystals. Furthermore, like the full-length ectodomain of TLR4, the longest TV8 hybrid could be multimerized by LPS (details in the section "Dimerization of the TLR4 and MD-2 complex"). From the analysis of the hybrid structures, we were convinced that the Hybrid LRR Technique did not cause substantial structural changes (See below "Structural rigidity of the LRR modules in the TLR4-VLR hybrids" section) and the complete structure of the ectodomain of human TLR4 was generated by aligning the overlapping regions of the TV8 and VT3 structures (Figure 4).

Structure of the TLR4-MD-2-Eritoran Complex

Among the hybrids, MD-2-bound TV3 was successfully crystallized with Eritoran and their complex structure was solved (Figure 5). Eritoran binds to the hydrophobic pocket in human MD-2, and there is no direct interaction between Eritoran and TLR4. The structure formed by the four acyl chains of Eritoran complements the shape of the hydrophobic pocket and snuggly occupies almost 90% of the solvent-accessible volume of the pocket, leaving only a narrow groove near its opening (Figures 5B and 5C). Although the R2 and R3 acyl chains adopt a fully

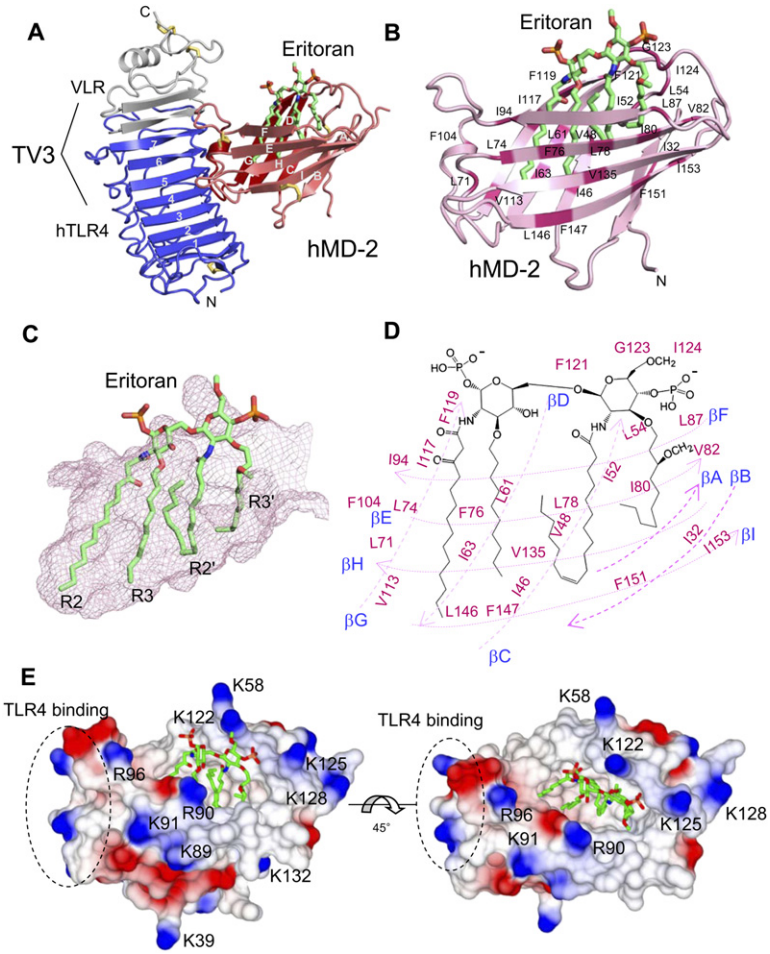

Figure 5. Structure of the TLR4-MD-2-Eritoran Complex

(A) Overall structure of the TV3-hMD-2-Eritoran complex. The TLR4 part of TV3 is colored blue and the VLR part gray.

(B) Closeup view of the human MD-2 and Eritoran complex. The bound TV3 hybrid is omitted for clarity. The carbon, oxygen, and phosphorous atoms of Eritoran are green, red, and orange, respectively. MD-2 residues interacting with the hydrophobic acyl chains of Eritoran are colored magenta and labeled.

(C) Shape of the Eritoran-binding pocket. The surface of MD-2 is drawn in purple mesh. The four acyl chains of Eritoran are labeled.

(D) Chemical structure of Eritoran. MD-2 residues interacting with Eritoran are labeled. The β strands are shown schematically as broken arrows.

(E) Surface representation of MD-2. Positively and negatively charged surfaces are colored blue and red, respectively. Lysines and arginines interacting ionically with Eritoran are labeled. The bound TV3 hybrid is omitted for clarity.

extended conformation, the R2′ and R3′ acyl chains are bent in the middle (Figure 5C). The double bond of the R2′ acyl chain has a *cis* conformation, and the chain makes a 180 degree turn at the *cis* double bond to occupy the empty space in the pocket (Figure 5D).

The di-glucosamine backbone of Eritoran conserved in all LPS molecules is fully exposed to solvent. Although the di-glucosamine sugars do not interact directly with MD-2, the two phosphate groups attached to the backbone form ionic bonds with several positively charged residues located at the opening of the pocket (Figures 5D and 5E). This is consistent with biochemical studies showing that the di-glucosamine groups are dispensable for binding of synthetic ligands derived from LPS to MD-2, whereas the phosphate groups are essential (Brandenburg et al., 2004).

The TV3 hybrid does not contain the B patch but still forms a stable complex with MD-2, suggesting that the A patch of TLR4 plays the major role in MD-2 interaction. This is consistent with the evolutionary analysis of TLR4 where the A patch shows higher conservation than the B patch (Figure 3C). All the residues involved in the A-A′ patch interaction are present in the TV3-MD-2 complex, and deletion of the B patch induces no substantial structural changes in the interaction of the A and A′ patches.

Structural Comparison of TLR4 and MD-2 with Related Proteins

We compared the structures of mouse TLR4 in complex with MD-2 and the human TLR4 without bound MD-2. Mouse and human TLR4 have 62.4% sequence identity and therefore are expected to have highly homologous structures. Indeed, the N- and C-terminal domains of the two TLR4 structures could be superimposed with average Cα rms differences of 0.66 Å and 1.56 Å, respectively (Figure S2). The largest structural differences of the C-terminal domain were located in the LRRCT module, where the insertion of Glu563 in human TLR4 caused a 3.5 Å displacement of the LRRCT module.

The central domains differ substantially more in structure than the N- and C-terminal domains. MD-2-bound mouse TLR4 has its LRR9 loop shifted by more than 12 Å, which bends the entire horseshoe-like structure by approximately 20 degrees. The observed structural change is unlikely to be due to the sequence differences between human and mouse TLR4 central domains. These are 56% identical, and residues with clear structural roles are strictly conserved. Instead, the structural change is likely to be caused by MD-2 binding because the LRR9 loop of mouse TLR4 occupies the central region of the B

patch and interacts at many points with MD-2 (Figure 3A). Future crystallographic experiments using MD-2-free mouse TLR4 are required to confirm the origin of the structural changes in the central domain.

Mouse and human MD-2 share 64% sequence identity. As expected, the two MD-2 structures show high structural homology with a Cα rms difference of 1.2 Å (Figure S3A). It should be noted that our mouse MD-2 is complexed with the full-length ectodomain of mouse TLR4 but without any bound ligands, whereas human MD-2 is complexed with the shorter TV3 hybrid and Eritoran. Except for small shifts in the B′ patch and the loops between the βG-βH and βA-βB strands, binding of Eritoran or deletion of the B patch in TV3 did not induce significant structural changes in MD-2. Lipid IVa is the precursor form of lipid A. It has an antagonistic effect on human TLR4-MD-2 but an agonistic effect on the mouse TLR4-MD-2 complex. Both MD-2 and TLR4 have been reported to be important for the species-specific response to lipid IVa (Lien et al., 2000; Muroi and Tanamoto, 2006; Poltorak et al., 2000). The residues important for the species-specific response are Thr57, Val61, and Glu122 of mouse MD-2 (Muroi and Tanamoto, 2006). In our crystal structure, they show only minor structural changes between human and mouse MD-2s, suggesting that subtle structural changes in MD-2 may have a significant impact on activation of TLR4-MD-2 (Figure S3B).

MD-2 shares the β cup topology with the ML family of lipid-binding proteins (Gruber et al., 2004; Inohara and Nunez, 2002). A search of the structural neighborhood of MD-2 in the Dali database yielded GM2 activator protein and NPC2 at the top, with Z values of 7.5 and 6.3, respectively (Figure S4). The ML family proteins have two antiparallel β sheets and conserved disulfide bridges (Derewenda et al., 2002; Friedland et al., 2003; Wright et al., 2003). However, the structural similarity between MD-2 and other ML family proteins is restricted to the overall connectivity of the β strands, and the MD-2 structure could not be superimposed on any of the ML family proteins; MD-2 has more β strands and a larger ligand-binding pocket. The shape of the ligand-binding pocket of MD-2 suggests that it has evolved to accommodate large and structurally diverse ligands.

Dimerization of the TLR4 and MD-2 Complex

It has been reported that binding of agonistic LPS induces aggregation of TLR4 and initiates intracellular signaling (Kobayashi et al., 2006; Prohinar et al., 2007). To further characterize the structural properties of the TLR4 multimer, we investigated the aggregation state of purified TLR4-MD-2 after binding LPS, using gel filtration chromatography, native gel electrophoresis, and crosslinking experiments (Figures 6A–6C). Binding of Eritoran to the full-length ectodomains of mouse and human TLR4-MD-2 did not alter their elution volumes in gel filtration chromatography and caused only small changes in migration speed in native gel electrophoresis (Figures 6A and 6B). In contrast, binding of LPS caused large changes in the aggregation state of the TLR4-MD-2 complexes. LPS-bound TLR4-MD-2 eluted earlier in gel filtration chromatography and shifted upwards in native gel electrophoresis. The elution volume of the LPS-bound protein complex in the gel filtration chromatography was consistent with the predicted elution volume of a TLR4-MD-2 heterotetramer (Figure 6A). Furthermore, the LPS-bound TLR4-MD-2 formed a band consistent with the size of the TLR4-MD-2 heterotetramer after crosslinking with glutaraldehyde and SDS gel electrophoresis (Figure 6C). The central and/or C-terminal domains of TLR4 are required for the receptor dimerization because the TV3 hybrid that contains only the N-terminal domain and a part of the central domain interacts normally with MD-2 but did not form a heterotetramer after LPS binding (Figures 6A and 6B). On the other hand, the TV8 hybrid composed of the N-terminal, the central, and 75% of the C-terminal domain behaved similarly with the full-length ectodomain TLR4 in LPS-induced multimerization. Collectively, these experiments demonstrate that LPS, but not Eritoran, causes dimerization of the TLR4-MD-2 complex, and that dimerization requires the central and/or the C-terminal domains of TLR4.

To locate the residues of MD-2 involved in dimerization we performed site-directed mutagenesis experiments. Kobayashi et al. have shown that mutations of Phe126 and Gly129 in mouse MD-2 prevent aggregation of the TLR4-MD-2 complex (Kobayashi et al., 2006). These residues are both opposite to the TLR-4-binding site of MD-2 (Figure 6D). To further characterize this Phe126 edge of MD-2, we conducted additional mutagenesis experiments. Phe126 and His155 mutants of MD-2 bound as normal to TLR4 and LPS, but their complex with TLR4 was not dimerized by LPS (Figure 6E). Although the Val82 and Met85 residues are located close to Phe126 and His155, altering them by mutation did not affect multimerization of the TLR4-MD-2 complex; this finding confirms that the Phe126 and His155 residues play specific roles in receptor dimerization.

DISCUSSION

Model of LPS Bound to TLR4-MD-2

The mode of interaction of the TLR4-MD-2 complex with Eritoran reported in this article is likely to resemble that with LPS for the following reasons. (1) Because Eritoran competes with LPS for binding to MD-2 (Visintin et al., 2005), their binding sites must at least overlap. (2) Eritoran is derived from the lipid A structure of *Rhodobacter sphaeroides* LPS. The di-glucosamine backbone is conserved and the lipid chains are very similar in chemical structure (Rossignol and Lynn, 2005). (3) Recently Ohto et al. reported a crystal structure of human MD-2 in complex with lipid IVa (Ohto et al., 2007). In their and our MD-2 structures, lipid IVa and Eritoran bind to the same area in MD-2 (Figure S5). The bound di-glucosamine backbone and the lipid chains of lipid IVa show small but interesting

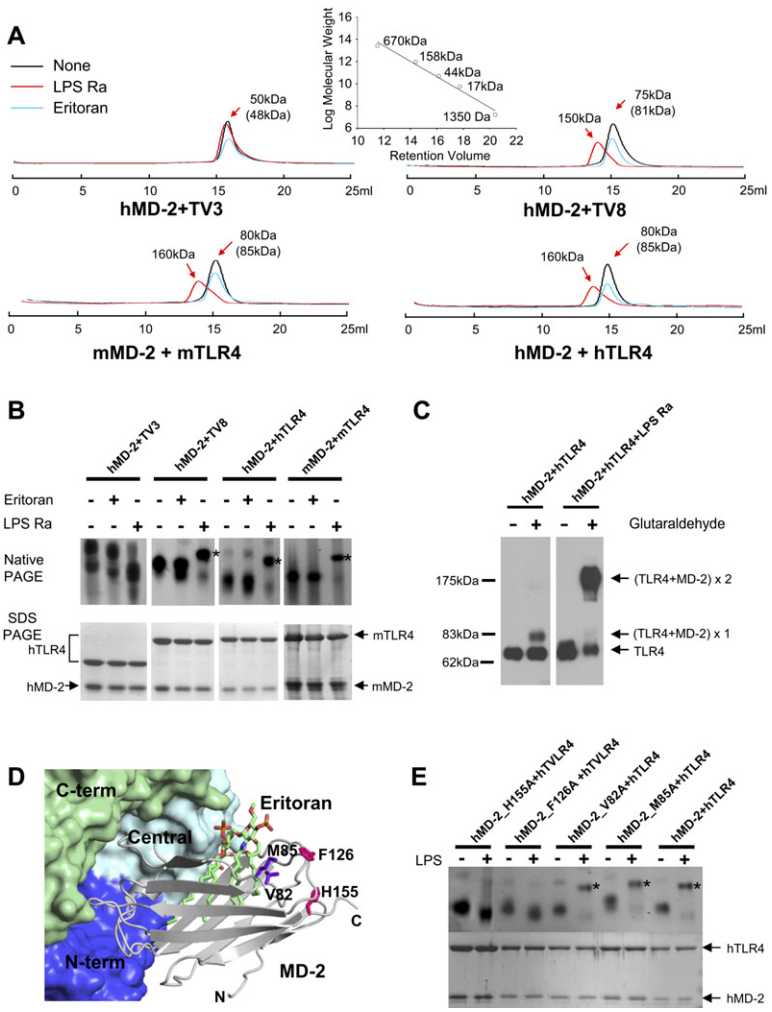

Figure 6. Dimerization of the TLR4-MD-2 Complex

(A) Gel filtration chromatography of the TLR4-MD-2 complexes. Full-length and hybrid TLR4 proteins in complex with MD-2 were incubated with LPS Ra or Eritoran and analyzed by Superdex 200 gel filtration chromatography, calibrated with molecular weight standards. The apparent molecular weights of the complexes calculated from the elution volumes are shown, and the expected molecular weights of the monomeric TLR4-MD-2 complexes are given in parentheses.

(B) Native and SDS-PAGE analysis of the TLR4-MD-2 complexes. The TLR4-MD-2 complexes were incubated with Eritoran or *E. coli* LPS Ra and analyzed. Dimerized complexes migrate more slowly than the monomeric complex and are marked with *. The Eritoran-bound protein complexes run slightly faster than the unbound complexes due to the negative charges on the ligand.

(C) Glutaraldehyde crosslinking of the TLR4-MD-2 complex. The TLR4-MD-2 complex not bound to LPS (left lanes) was crosslinked as a monomeric TLR4-MD-2 complex with the expected molecular weight of 85 kDa. The LPS-bound TLR4-MD-2 complex was crosslinked as a dimer with the expected molecular weight of 170 kDa.

(D) Positions of the Phe126 and His155 residues. These residues are located on the opposite side of TLR4. The full-length ectodomain of TLR4 was modeled by superimposing the TV3 and mouse TLR4 structures and its surfaces are shown in blue, cyan, and green.

(E) Dimerization of the mutant MD-2 s with TLR4 and LPS Ra. TLR4 and mutant MD-2 complexes were incubated with *E. coli* LPS Ra and analyzed by native gel electrophoresis. The dimerized protein complexes run more slowly than the monomeric protein complex and are marked with *.

structural changes compared to those of Eritoran. (4) All ML family proteins are small and have only one ligand-binding pocket. The Eritoran-binding pocket of MD-2 is located in the same region where GM2 activator protein, Der P2, and NPC2 have been proposed to interact with their ligands (Derewenda et al., 2002; Friedland et al., 2003; Wright et al., 2003). (5) Previous mutagenesis results demonstrate that several residues involved in Eritoran binding also play indispensable roles in LPS binding. Lys89, Arg90, Lys91, Lys122, Lys125, Lys128, and Lys132, which are reported to be essential for LPS binding and NFκB activation, are located near the opening of the Eritoran-binding pocket and interact ionically with the phosphate groups in Eritoran (Figure 5E) (Gruber et al., 2004; Re and Strominger, 2003; Visintin et al., 2003).

Although Eritoran has a clear structural resemblance to LPS, they have opposite physiological effects: Eritoran is an antagonist and LPS an agonist. Therefore, there must be significant differences in their modes of interaction. The length and number of acyl chains in natural LPS vary between bacterial species and appear to be strongly correlated with agonist strength (Teghanemt et al., 2005). *E. coli* and *Salmonella* LPSs usually have six acyl chains and are strong agonists of TLR4. Since the four acyl chains of Eritoran occupy almost all the available space in the MD-2 pocket, significant structural changes of the pocket appear to be inevitable when more, or longer, acyl chains are accommodated. These structural changes in MD-2 induced by LPS binding may reveal an otherwise hidden binding site required for aggregation and activation of the TLR4-MD-2 complex.

Model of the LPS-Induced TLR4-MD-2 Dimerization

The mutagenesis data reported by us and by Kobayashi et al. show that the Phe126 edge of MD-2 mediates the aggregation of the TLR4-MD-2 complex (Kobayashi

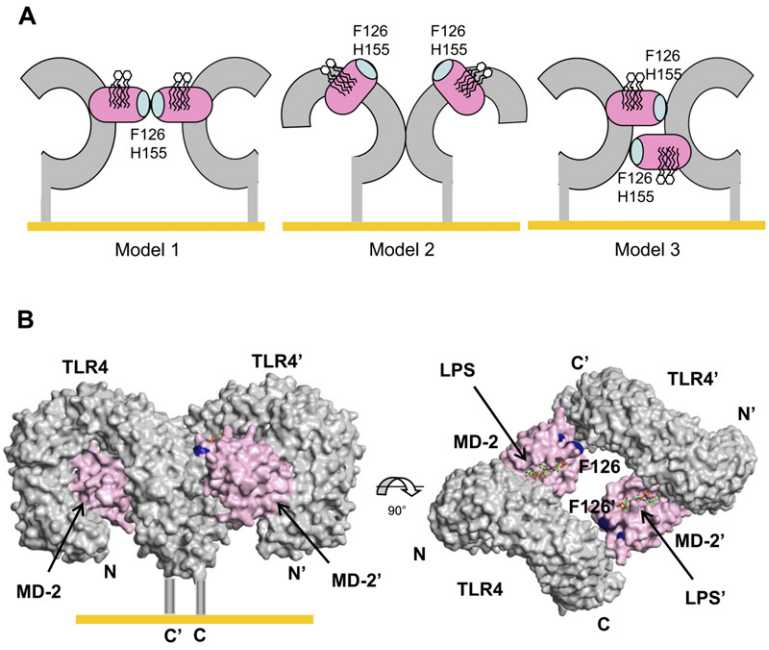

Figure 7. Model of the TLR4-MD-2 Dimer

(A) Three models of the TLR4-MD-2 dimer are shown. MD-2 and TLR4 are colored in magenta and gray, respectively. The yellow bars represent the cell membrane.

(B) Three-dimensional representation of Model 3. Surfaces of TLR4 and MD-2 are gray and magenta, respectively. The Phe126 and His155 residues important for dimerization are blue. The labels that belong to the second TLR4-MD-2 complex are marked with apostrophes.

et al., 2006). We also found that receptor dimerization requires the central and/or C-terminal domain of TLR4. Three models of receptor dimerization are shown in Figure 7A. In the first model, LPS binding induces a structural change in the Phe126 edge of MD-2, which then makes direct contact with a second MD-2 molecule. This model cannot explain why the central or C-terminal domain of TLR4 is required for receptor dimerization. In the second model, LPS binding to MD-2 induces a structural change in TLR4 and promotes direct dimerization of TLR4 molecules. This model cannot explain why mutations in the Phe126 edge of MD-2, which is located on the opposite side of TLR4, block receptor dimerization. The possibility of a long-range effect of the MD-2 mutations by inducing conformational changes of TLR4 cannot be excluded but is very unlikely considering the unusually high structural rigidity of the LRR modules in TLR4 (see next section). In the favored third model, LPS binding induces a structural change in the Phe126 edge of MD-2 that promotes interaction between the edge and the central or C-terminal domain of a second TLR4. A three-dimensional view of model 3 demonstrates that the intracellular TIR domains can form close contact (Figure 7B).

CD14 is indispensable for physiological response of LPS by catalyzing binding of LPS to the TLR4-MD-2 complex and by modulating signaling activity of LPS (Haziot et al., 1995; Jiang et al., 2005; Miyake, 2006). Mutations of CD14 that block LPS transfer to TLR4-MD-2 are clustered in one face of CD14 near its LPS-binding pocket (Kim et al., 2005). Future biochemical and structural research is required to identify a CD14 interaction site in TLR4-MD-2 and the mechanism of LPS transfer from CD14 to TLR4-MD-2.

Structural Rigidity of the LRR Modules in the TLR4-VLR Hybrids

Since the structures of proteins adapt to the environments provided by their sequences, our primary concern while designing the TLR4-VLR hybrids was that fusion might lead to unpredictable structural changes of the TLR4 or VLR modules. We previously solved the crystal structures of several VLR clones of Pacific hagfish (Kim et al., 2007). To check for the presence of structural changes in the VLR modules, we superimposed the structure of native VLRB.61 on those of the VLR modules of the hybrid proteins (Figure S6). The backbone atoms of the native and hybrid proteins had practically identical structures, with an average Cα rms difference of 0.3 ~0.4 Å after superimposition. Since we did not know the structure of full-length human TLR4, we could not directly compare the hybrid structures to the structure of TLR4. Instead, we compared the structures of the overlapping regions of the three TLR hybrids. The entire length of the TLR4 fragment in the TV3 hybrid is included in the longer TV8 hybrids, and 145 residues from amino acid 383 to 527 are common to the VT3 and the TV8 hybrids (Table S2). The overlapping regions have practically identical backbone structures with average Cα rms differences of 0.39 Å and 0.28 Å, respectively (Figure S7). As a control, TLR3 structures determined independently by two research groups were superimposed, and their average Cα rms difference was 1.1 Å (Bell et al., 2005; Choe et al., 2005). Surprisingly, the structural homology is not restricted to the backbone atoms; even at the fusion site the side chains have similar conformations, apart from the long and flexible ones. The unexpected structural rigidity of the LRR modules is surprising but understandable since the concave β strand region of LRR

proteins is an unusually rigid structural frame. From the analysis described above, we were convinced that the Hybrid LRR Technique did not cause substantial structural changes.

Applications of the Hybrid LRR Technique

The Hybrid LRR Technique made two crucial contributions to our structural studies on the TLR4-MD-2 system. (1) It was essential for crystallizing TLR4-MD-2 with bound Eritoran. The mouse TLR4-MD-2 complex could not be crystallized with LPS or LPS analogs, which made biological interpretation of the structural results very difficult. To solve this problem, we continued to generate new hybrids until we found one that could be crystallized with bound ligands. The TV3 hybrid was the first to be crystallized with MD-2 and Eritoran, and its structure was determined. (2) The hybrid proteins were useful for structure determination. Although the mouse TLR4-MD-2 complex was crystallized successfully, structure determination by molecular replacement using the TLR3 structure was not possible due to substantial structural differences between TLR3 and TLR4. However, the short TV3 hybrid had considerable structural homology with the N-terminal portion of TLR3, and its structure could be solved by molecular replacement using the reported TLR3 and VLR structures as search probes. The refined structure of TV3 in turn served as a good search probe for longer TLR4 fragments. Furthermore, crystals of the smaller hybrid proteins tended to diffract X-rays to high resolution, which greatly simplified structure determination.

The Hybrid LRR Technique may have broader applications. It can be used to reduce the size of proteins to the minimum required for function. It can also be applied to generate multifunctional LRR proteins. For example, it may be possible to design hybrid proteins with both TLR4 and TLR2 activities. Such artificial proteins may have beneficial properties as therapeutic reagents. Fusion strategies similar to the Hybrid LRR Technique may be applicable to other repeat families such as the ankyrin or WD40 repeat proteins.

In conclusion, we report the first crystal structures of human and mouse TLR4-MD-2 complexes. Eritoran, an antagonistic homolog of LPS, binds to a large internal pocket in MD-2. Based on mutagenesis experiments on MD-2 and TLR4, we propose a model of TLR4-MD-2 dimerization induced by LPS. The Hybrid LRR Technique was needed for crystallographic study of TLR4-MD-2 and may have broader applications in biological studies of LRR family proteins and their medical uses.

EXPERIMENTAL PROCEDURES

Protein Expression and Purification

The human TLR4-VLR hybrids (Table S2) were cloned into the BamHI and NotI sites of pAcGP67 vector (BD Biosciences) by overlap PCR using the primers listed in Table S3. The Fc domain of human IgG1 and a thrombin cleavage site was cloned between the NotI and the BglII sites of pAcGP67. The resulting Fc-tagged hybrids were expressed in Hi5 insect cells (Invitrogen) and purified by protein A Sepharose (GE Healthcare) affinity chromatography. After cleavage by thrombin to remove the Fc tag, the hybrid proteins were further purified by ion exchange and gel filtration chromatography (Table S4). The wild-type and mutant MD-2s fused to a protein A tag were coexpressed with TLR4 or TLR4-VLR hybrids in Hi5 cells and purified by IgG Sepharose (GE Healthcare) affinity chromatography. The protein A tag was removed by thrombin digestion and the TLR4-MD-2 complexes were further purified by ion exchange and gel filtration chromatography (Table S4).

Binding of LPS or Eritoran to the TLR4-MD-2 Complexes

E. coli LPS Ra (Sigma, L9641) or Eritoran were sonicated for 10 min and incubated with the TLR4-MD-2 complexes at 37°C for 3 hr. Eritoran was a generous gift from Eisai, Inc. The molar ratio of LPS or Eritoran to the protein was kept at 10:1. The TV3-MD-2-Eritoran complex used for crystallization was purified by Superdex-200 gel filtration chromatography (GE Healthcare) to remove unbound Eritoran. Native PAGE experiments were repeated using ultrapure LPS from List Biological Lab. The LPS-bound protein bands were similarly upward shifted but in multiple bands due to heterogeneity of LPS (data not shown). Ra mutant form of LPS does not contain O-antigen sugar groups and has lower heterogeneity. Addition of CD14 and LBP to the reaction mixture sped up the reaction but did not change in yield and aggregation state of the final products.

Crystallization and Data Collection

Crystals were grown for one week using the hanging-drop vapor diffusion method by mixing 1 μl of protein solution and 1 μl of crystallization buffer. The optimized crystallization conditions are summarized in Table S4. For data collection, the crystals were flash-frozen at −170°C in freezing buffers (Table S4). Diffraction data were collected at the 4A beam line of Pohang Accelerator Laboratory, the BL41XU beam line of SPring-8, or the ID14-2 beam line of ESRF. The HKL2000 package (Otwinowski and Minor, 1997) and the MOSFLM/SCALA (Winn, 2003) programs were used to index, integrate, and scale the diffraction data.

Structure Determination and Refinement

Initial phases were calculated by molecular replacement using the program PHASER (McCoy et al., 2005). The search probes used for the calculation are summarized in Table S5. Atomic models were built by iterative modeling and refinement using the program O and CNS (Brunger et al., 1998; Jones et al., 1991). Atomic model of Eritoran was built into a strong and continuous electron density that was found in the MD-2 pocket (Figure S8). The final models were further refined using the program REFMAC (Murshudov et al., 1997) with the TLS program parameters generated by the TLSMD server (Painter and Merritt, 2006). No nonglycine residues are found in the disallowed regions of the Ramachandran plots.

Supplemental Data

Supplemental Data include Supplemental Experimental Procedures, eight figures, five tables, and references and can be found with this article online at http://www.cell.com/cgi/content/full/130/5/906/DC1/.

ACKNOWLEDGMENTS

We thank the staff of the Pohang Accelerator Laboratory, Spring-8, and ESRF for help with data collection. We thank Dr. Julian Gross for critical reading of the manuscript. This work was supported by the Molecular and Cellular BioDiscovery Program and the Functional Proteomics Program (FPR05B2-140) from the Ministry of Science of Korea.

Received: June 22, 2007
Revised: July 23, 2007
Accepted: August 2, 2007
Published: September 6, 2007

REFERENCES

Bell, J.K., Botos, I., Hall, P.R., Askins, J., Shiloach, J., Segal, D.M., and Davies, D.R. (2005). The molecular structure of the Toll-like receptor 3 ligand-binding domain. Proc. Natl. Acad. Sci. USA *102*, 10976–10980.

Brandenburg, K., Hawkins, L., Garidel, P., Andra, J., Muller, M., Heine, H., Koch, M.H., and Seydel, U. (2004). Structural polymorphism and endotoxic activity of synthetic phospholipid-like amphiphiles. Biochemistry *43*, 4039–4046.

Brunger, A.T., Adams, P.D., Clore, G.M., DeLano, W.L., Gros, P., Grosse-Kunstleve, R.W., Jiang, J.S., Kuszewski, J., Nilges, M., Pannu, N.S., et al. (1998). Crystallography & NMR system: A new software suite for macromolecular structure determination. Acta Crystallogr. D Biol. Crystallogr. *54*, 905–921.

Choe, J., Kelker, M.S., and Wilson, I.A. (2005). Crystal structure of human toll-like receptor 3 (TLR3) ectodomain. Science *309*, 581–585.

Derewenda, U., Li, J., Derewenda, Z., Dauter, Z., Mueller, G.A., Rule, G.S., and Benjamin, D.C. (2002). The crystal structure of a major dust mite allergen Der p 2, and its biological implications. J. Mol. Biol. *318*, 189–197.

Friedland, N., Liou, H.L., Lobel, P., and Stock, A.M. (2003). Structure of a cholesterol-binding protein deficient in Niemann-Pick type C2 disease. Proc. Natl. Acad. Sci. USA *100*, 2512–2517.

Gay, N.J., and Gangloff, M. (2007). Structure and function of toll receptors and their ligands. Annu. Rev. Biochem. *76*, 141–165.

Gioannini, T.L., Teghanemt, A., Zhang, D., Coussens, N.P., Dockstader, W., Ramaswamy, S., and Weiss, J.P. (2004). Isolation of an endotoxin-MD-2 complex that produces Toll-like receptor 4-dependent cell activation at picomolar concentrations. Proc. Natl. Acad. Sci. USA *101*, 4186–4191.

Gioannini, T.L., Teghanemt, A., Zhang, D., Levis, E.N., and Weiss, J.P. (2005). Monomeric endotoxin:protein complexes are essential for TLR4-dependent cell activation. J. Endotoxin Res. *11*, 117–123.

Gruber, A., Mancek, M., Wagner, H., Kirschning, C.J., and Jerala, R. (2004). Structural model of MD-2 and functional role of its basic amino acid clusters involved in cellular lipopolysaccharide recognition. J. Biol. Chem. *279*, 28475–28482.

Hajjar, A.M., Ernst, R.K., Tsai, J.H., Wilson, C.B., and Miller, S.I. (2002). Human Toll-like receptor 4 recognizes host-specific LPS modifications. Nat. Immunol. *3*, 354–359.

Haziot, A., Ferrero, E., Lin, X.Y., Stewart, C.L., and Goyert, S.M. (1995). CD14-deficient mice are exquisitely insensitive to the effects of LPS. Prog. Clin. Biol. Res. *392*, 349–351.

He, X.L., Bazan, J.F., McDermott, G., Park, J.B., Wang, K., Tessier-Lavigne, M., He, Z., and Garcia, K.C. (2003). Structure of the Nogo receptor ectodomain: a recognition module implicated in myelin inhibition. Neuron *38*, 177–185.

Hoshino, K., Takeuchi, O., Kawai, T., Sanjo, H., Ogawa, T., Takeda, Y., Takeda, K., and Akira, S. (1999). Cutting edge: Toll-like receptor 4 (TLR4)-deficient mice are hyporesponsive to lipopolysaccharide: evidence for TLR4 as the Lps gene product. J. Immunol. *162*, 3749–3752.

Hyakushima, N., Mitsuzawa, H., Nishitani, C., Sano, H., Kuronuma, K., Konishi, M., Himi, T., Miyake, K., and Kuroki, Y. (2004). Interaction of soluble form of recombinant extracellular TLR4 domain with MD-2 enables lipopolysaccharide binding and attenuates TLR4-mediated signaling. J. Immunol. *173*, 6949–6954.

Inohara, N., and Nunez, G. (2002). ML–a conserved domain involved in innate immunity and lipid metabolism. Trends Biochem. Sci. *27*, 219–221.

Jiang, Z., Georgel, P., Du, X., Shamel, L., Sovath, S., Mudd, S., Huber, M., Kalis, C., Keck, S., Galanos, C., et al. (2005). CD14 is required for MyD88-independent LPS signaling. Nat. Immunol. *6*, 565–570.

Jones, T.A., Zou, J.Y., Cowan, S.W., and Kjeldgaard. (1991). Improved methods for building protein models in electron density maps and the location of errors in these models. Acta Crystallogr. A *47*, 110–119.

Kajava, A.V. (1998). Structural diversity of leucine-rich repeat proteins. J. Mol. Biol. *277*, 519–527.

Kim, H.M., Oh, S.C., Lim, K.J., Kasamatsu, J., Heo, J.Y., Park, B.S., Lee, H., Yoo, O.J., Kasahara, M., and Lee, J.O. (2007). Structural diversity of the hagfish variable lymphocyte receptors. J. Biol. Chem. *282*, 6726–6732.

Kim, J.I., Lee, C.J., Jin, M.S., Lee, C.H., Paik, S.G., Lee, H., and Lee, J.O. (2005). Crystal structure of CD14 and its implications for lipopolysaccharide signaling. J. Biol. Chem. *280*, 11347–11351.

Kobayashi, M., Saitoh, S., Tanimura, N., Takahashi, K., Kawasaki, K., Nishijima, M., Fujimoto, Y., Fukase, K., Akashi-Takamura, S., and Miyake, K. (2006). Regulatory roles for MD-2 and TLR4 in ligand-induced receptor clustering. J. Immunol. *176*, 6211–6218.

Kobe, B., and Kajava, A.V. (2001). The leucine-rich repeat as a protein recognition motif. Curr. Opin. Struct. Biol. *11*, 725–732.

Landau, M., Mayrose, I., Rosenberg, Y., Glaser, F., Martz, E., Pupko, T., and Ben-Tal, N. (2005). ConSurf 2005: the projection of evolutionary conservation scores of residues on protein structures. Nucleic Acids Res. *33*, W299–W302.

Lien, E., Means, T.K., Heine, H., Yoshimura, A., Kusumoto, S., Fukase, K., Fenton, M.J., Oikawa, M., Qureshi, N., Monks, B., et al. (2000). Toll-like receptor 4 imparts ligand-specific recognition of bacterial lipopolysaccharide. J. Clin. Invest. *105*, 497–504.

Matsushima, N., Tanaka, T., Enkhbaya, P., Mikami, T., Taga, M., Ymada, K., and Kuroki, Y. (2007). Comparative sequence analysis of leucine-rich repeats (LRRs) within vertebrate toll-like receptors. BMC Genomics *8*, 124.

McCoy, A.J., Grosse-Kunstleve, R.W., Storoni, L.C., and Read, R.J. (2005). Likelihood-enhanced fast translation functions. Acta Crystallogr. D Biol. Crystallogr. *61*, 458–464.

Medzhitov, R., Preston-Hurlburt, P., and Janeway, C.A., Jr. (1997). A human homologue of the Drosophila Toll protein signals activation of adaptive immunity. Nature *388*, 394–397.

Miyake, K. (2006). Roles for accessory molecules in microbial recognition by Toll-like receptors. J. Endotoxin Res. *12*, 195–204.

Mullarkey, M., Rose, J.R., Bristol, J., Kawata, T., Kimura, A., Kobayashi, S., Przetak, M., Chow, J., Gusovsky, F., Christ, W.J., and Rossignol, D.P. (2003). Inhibition of endotoxin response by e5564, a novel Toll-like receptor 4-directed endotoxin antagonist. J. Pharmacol. Exp. Ther. *304*, 1093–1102.

Muroi, M., and Tanamoto, K. (2006). Structural regions of MD-2 that determine the agonist-antagonist activity of lipid IVa. J. Biol. Chem. *281*, 5484–5491.

Murshudov, G.N., Vagin, A.A., and Dodson, E.J. (1997). Refinement of macromolecular structures by the maximum-likelihood method. Acta Crystallogr. D Biol. Crystallogr. *53*, 240–255.

Nagai, Y., Akashi, S., Nagafuku, M., Ogata, M., Iwakura, Y., Akira, S., Kitamura, T., Kosugi, A., Kimoto, M., and Miyake, K. (2002). Essential role of MD-2 in LPS responsiveness and TLR4 distribution. Nat. Immunol. *3*, 667–672.

Nishitani, C., Mitsuzawa, H., Hyakushima, N., Sano, H., Matsushima, N., and Kuroki, Y. (2005). The Toll-like receptor 4 region Glu24-Pro34 is critical for interaction with MD-2. Biochem. Biophys. Res. Commun. *328*, 586–590.

Nishitani, C., Mitsuzawa, H., Sano, H., Shimizu, T., Matsushima, N., and Kuroki, Y. (2006). Toll-like receptor 4 region Glu24-Lys47 is a site for MD-2 binding: importance of CYS29 and CYS40. J. Biol. Chem. *281*, 38322–38329.

Ohto, U., Fukase, K., Miyake, K., and Satow, Y. (2007). Crystal structures of human MD-2 and its complex with antiendotoxic lipid IVa. Science *316*, 1632–1634.

Otwinowski, Z., and Minor, W. (1997). Processing of X-ray diffraction data collected in oscillation mode. Methods Enzymol. *276*, 307–326.

Painter, J., and Merritt, E.A. (2006). Optimal description of a protein structure in terms of multiple groups undergoing TLS motion. Acta Crystallogr. D Biol. Crystallogr. *62*, 439–450.

Poltorak, A., He, X., Smirnova, I., Liu, M.Y., Van Huffel, C., Du, X., Birdwell, D., Alejos, E., Silva, M., Galanos, C., et al. (1998). Defective LPS signaling in C3H/HeJ and C57BL/10ScCr mice: mutations in Tlr4 gene. Science *282*, 2085–2088.

Poltorak, A., Ricciardi-Castagnoli, P., Citterio, S., and Beutler, B. (2000). Physical contact between lipopolysaccharide and toll-like receptor 4 revealed by genetic complementation. Proc. Natl. Acad. Sci. USA *97*, 2163–2167.

Potterton, L., McNicholas, S., Krissinel, E., Gruber, J., Cowtan, K., Emsley, P., Murshudov, G.N., Cohen, S., Perrakis, A., and Noble, M. (2004). Developments in the CCP4 molecular-graphics project. Acta Crystallogr. D Biol. Crystallogr. *60*, 2288–2294.

Prohinar, P., Re, F., Widstrom, R., Zhang, D., Teghanemt, A., Weiss, J.P., and Gioannini, T.L. (2007). Specific high affinity interactions of monomeric endotoxin.protein complexes with Toll-like receptor 4 ectodomain. J. Biol. Chem. *282*, 1010–1017.

Qureshi, S.T., Lariviere, L., Leveque, G., Clermont, S., Moore, K.J., Gros, P., and Malo, D. (1999). Endotoxin-tolerant mice have mutations in Toll-like receptor 4 (Tlr4). J. Exp. Med. *189*, 615–625.

Raetz, C.R., and Whitfield, C. (2002). Lipopolysaccharide endotoxins. Annu. Rev. Biochem. *71*, 635–700.

Re, F., and Strominger, J.L. (2002). Monomeric recombinant MD-2 binds toll-like receptor 4 tightly and confers lipopolysaccharide responsiveness. J. Biol. Chem. *277*, 23427–23432.

Re, F., and Strominger, J.L. (2003). Separate functional domains of human MD-2 mediate Toll-like receptor 4-binding and lipopolysaccharide responsiveness. J. Immunol. *171*, 5272–5276.

Roach, J.C., Glusman, G., Rowen, L., Kaur, A., Purcell, M.K., Smith, K.D., Hood, L.E., and Aderem, A. (2005). The evolution of vertebrate Toll-like receptors. Proc. Natl. Acad. Sci. USA *102*, 9577–9582.

Rossignol, D.P., and Lynn, M. (2005). TLR4 antagonists for endotoxemia and beyond. Curr. Opin. Investig. Drugs *6*, 496–502.

Schromm, A.B., Lien, E., Henneke, P., Chow, J.C., Yoshimura, A., Heine, H., Latz, E., Monks, B.G., Schwartz, D.A., Miyake, K., and Golenbock, D.T. (2001). Molecular genetic analysis of an endotoxin nonresponder mutant cell line: a point mutation in a conserved region of MD-2 abolishes endotoxin-induced signaling. J. Exp. Med. *194*, 79–88.

Shimazu, R., Akashi, S., Ogata, H., Nagai, Y., Fukudome, K., Miyake, K., and Kimoto, M. (1999). MD-2, a molecule that confers lipopolysaccharide responsiveness on Toll-like receptor 4. J. Exp. Med. *189*, 1777–1782.

Teghanemt, A., Zhang, D., Levis, E.N., Weiss, J.P., and Gioannini, T.L. (2005). Molecular basis of reduced potency of underacylated endotoxins. J. Immunol. *175*, 4669–4676.

Viriyakosol, S., Tobias, P.S., Kitchens, R.L., and Kirkland, T.N. (2001). MD-2 binds to bacterial lipopolysaccharide. J. Biol. Chem. *276*, 38044–38051.

Visintin, A., Latz, E., Monks, B.G., Espevik, T., and Golenbock, D.T. (2003). Lysines 128 and 132 enable lipopolysaccharide binding to MD-2, leading to Toll-like receptor-4 aggregation and signal transduction. J. Biol. Chem. *278*, 48313–48320.

Visintin, A., Halmen, K.A., Latz, E., Monks, B.G., and Golenbock, D.T. (2005). Pharmacological inhibition of endotoxin responses is achieved by targeting the TLR4 coreceptor, MD-2. J. Immunol. *175*, 6465–6472.

Winn, M.D. (2003). An overview of the CCP4 project in protein crystallography: an example of a collaborative project. J. Synchrotron Radiat. *10*, 23–25.

Wright, C.S., Zhao, Q., and Rastinejad, F. (2003). Structural analysis of lipid complexes of GM2-activator protein. J. Mol. Biol. *331*, 951–964.

Accession Numbers

The atomic coordinates of TV3, TV8, VT3, TV3-hMD-2-Eritoran, and mTLR4-mMD-2 have been deposited in the Protein Data Bank with the accession codes 2Z62, 2Z63, 2Z66, 2Z65, and 2Z64, respectively.